AIChE WILEY InterScience DISCOVER SOMETHING GREAT

MATERIALS, INTERFACES, AND ELECTROCHEMICAL PHENOMENA

Mechanism of Foaming on Polymer-Paperboard Composites

S. Kiran Annapragada
Institute of Paper Science and Technology, and School of Chemical and Biomolecular Engineering, Georgia Institute of Technology, 500 Tenth St NW, Atlanta, GA 30332

Timothy F. Patterson
Institute of Paper Science and Technology, and School of Mechanical Engineering, Georgia Institute of Technology, 500 Tenth St NW, Atlanta, GA 30332

Sujit Banerjee
Institute of Paper Science and Technology, and School of Chemical and Biomolecular Engineering, Georgia Institute of Technology, 500 Tenth St NW, Atlanta, GA 30332

DOI 10.1002/aic.11393
Published online December 10, 2007 in Wiley InterScience (www.interscience.wiley.com).

Foamed paperboard is a composite material with applications in the consumer products industry. The composite is comprised of paperboard sandwiched between two layers of polymers. One layer foams upon heating while the other acts as a barrier layer. Foaming is caused by the vaporization of the small amount of moisture present in the board and the resulting increase in pressure. The mechanism of foaming was investigated with a combination of high-speed photography, scanning electron microscopy, and infrared thermography using foamed paperboard of different compositions prepared both in the laboratory and on a commercial machine. The surface uniformity of the paper was found to be the overriding paper-related property controlling bubble formation. © 2007 American Institute of Chemical Engineers *AIChE J,* 54: 537–543, 2008
Keywords: bubble phenomena, foam, paper, polymer properties

Introduction

Foams generated from polymers are cellular plastics with gas bubbles dispersed in a polymeric matrix. They are light, low-cost, and have good thermal insulation and strength properties.[1–3] As a result, they are widely used in the food packaging and consumer products industries. Plastic foams do not degrade easily in the environment, and this, among other environmental considerations has prompted a search for alternatives. Foaming on paperboard is a relatively new technique that combines the advantages of traditional polymeric foam with the environmental benefits of paperboard. The paperboard is sandwiched between two polymers of different density. One face is foamed by the evaporating moisture in the board[4]; the other serves as a barrier. In effect, the moisture inside the paperboard replaces the blowing agent used in traditional foaming. The strength and insulation properties of the foam depend upon the nature of the polymer, the properties of the board, and the interactions between them. In this study we address the fundamental mechanism of foaming and identify the characteristics of the board that lead to a product with evenly distributed bubbles of a uniform size. This work is a first attempt to understand the fundamental mechanism of foaming on paper-polymer composites.

Methods and Materials

Handsheets (a term used to describe sheets prepared in the laboratory) were prepared in the laboratory at 250 g/m^2 from both southern hardwood and softwood bleached kraft pulps

Correspondence concerning this article should be addressed to S. Banerjee at sb@gatech.edu.

Table 1. Composition of Paper Boards Studied

Sample ID	Hardwood (%)	Softwood (%)	CSF (ml)	Filler (%)	Refining
M*	75	25	500	–	Jordan refiner
H1	100	0	300	–	Valley beater
H2	75	25	300	–	
H3	50	50	300	–	
H4	0	100	300	–	
H5	75	25	500	–	Jordan refiner
H6†	80	10,10	300	–	Valley beater
H7†	10,10	80	300	–	
H8‡	100	0	300	–	
H9‡	0	100	300	–	
H10	0	100	300	5	
H11	75	25	500	5	Jordan refiner

M, machine made paper; H, Handsheets.
*Sheets calendered.
†Stratified (multiply sheets).
‡Sheets extruded on felt side (all other handsheets extruded on wire side).

refined with a laboratory refiner and formed using a laboratory sheet former. Commercial machine-made samples were prepared on a full-scale paper machine. Additional samples (handsheets) were prepared from pulp refined commercially and formed using a laboratory sheet former. For the machine-made sheets, 11 kg of pulp were refined for 10 min at 6 net hp on a Jordan refiner to a freeness (a measure of drainage) of ~500 ml Canadian standard freeness (CSF). The sheets were pressed, dried, and calendered. Handsheets were prepared from various combinations of softwood and hardwood pulps refined in a Valley beater to a freeness of 300 ml CSF. In one instance, handsheets were prepared from the same pulp used to make the machine-made paper. In two instances, kaolin clay from Imerys (<2 μm) was added at 5% (based on fiber weight) to pulp suspensions used to make the handsheets. The laboratory formed sheets were prepared in a Formette Dynamique unit, which constructs a sheet layer-by-layer.[5,6] In contrast to the machine-made paper where the pulp suspension is sprayed on a moving wire where it drains and forms a mat, the Formette handsheet is prepared on a drum, which is sprayed continuously as it rotates. The mat is, therefore, built up incrementally.[5,6] The sheets were pressed at 7 kPa, and dried; Table 1 lists their compositions. All boards were extruded with a low density polyethylene (EC 482) of melt index (MI) 12 gm/10 min, density 0.918 gm/ml, and DSC melt temperature of 106°C obtained from Westlake Polymers.

During extrusion a thin film of molten thermoplastic polymer is pressed on to the paperboard through a slot die. Extrusion was done on one side of the sheet at a speed of 61 m/min to give a polymer layer thickness of 42.2 μm. For the handsheets, extrusion was done on the wire side of the sheet except for one case where the felt side was used. The opposite side of the sheet was sealed using a barrier layer as shown in Figure 1. This layer directs the vapor to the lower melt polymer (foaming) side. The barrier for the commercially prepared paperboards was a high-melting polyethylene; packaging tape was used for the handsheets. The higher melting PE (barrier layer) was a blend of HDPE and LDPE with melt temperatures above 132°C. Video images taken of the barrier layer confirmed that it remained intact during foaming. A heavy roller was used to expel any air trapped between the board and the tape. No significant difference in the number of bubbles was found when machine-made paper was foamed with either packaging tape or the extruded polyethylene as the barrier layer. In one instance, a lower melting packaging tape was employed to study the effects of barrier layer melting during foaming; the molten barrier led to poor foaming. The board-polymer composite was conditioned in a moisture-controlled room under TAPPI standard conditions of 50% relative humidity and 23°C until the moisture content reached 6–8%.[7] The boards were foamed in a convective oven at 132°C for 90 s.

Scanning electron microscope (SEM) images were collected with a LEO 1550 instrument. Cross-sections of the boards were imaged at various stages of foaming. Images were also collected from the surface of the board in order to measure x–y uniformity. Ten images were taken from different locations of each board and were analyzed using Image J software[8] obtained from the National Institutes of Health.

Bubble formation on the surface of the board was imaged at 100–2000 frames/s with a Phantom v4.2 high-speed camera from Vision Research. A combination of a Nikon Micro-Nikkon 105 mm f/2.8 lens and a bellows provided the required magnification. A length scale was obtained by taking a screen shot of a ruler placed in the focal plane of the camera. The area of observation at a resolution of 512 × 512 pixels was determined to be 5 × 5 mm. The light source was adjusted to be uniform across the area of interest.

The onset of foaming was indicated by the light reflected from the bubble surface as shown in Figure 2. The number of reflected light spots varied with the number and size of the bubbles formed. This correspondence between the light reflected and the number of bubbles was manually verified. Videos were recorded at 100 frames/s, and individual snapshots at different times were taken as well. Frames were

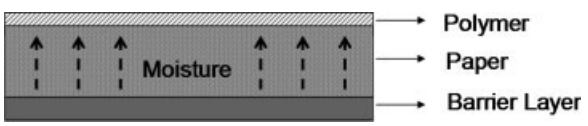

Figure 1. Schematic of the extruded board composite.

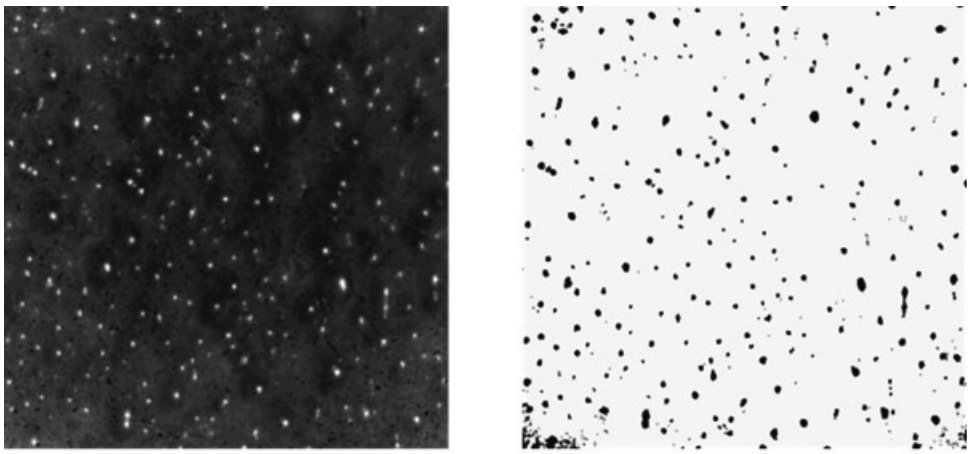

Figure 2. Images of bubbles: (a) original and (b) after processing.

grabbed from the beginning of the process until 90 s after the first bubble appeared in the video. The images were processed with Image J software to determine the rate of bubble growth. The brightness and contrast of each image was adjusted and a threshold value of between 10 and 255 pixel was set. This sequence is illustrated in Figure 2. Bubble growth causes a change in the focal point and is a potential source of error because of the very small depth of the field at the high magnifications. This needed constant manual adjusting of the lens/bellows combinations. All measurements were made at least in duplicate.

Infrared thermography was used to determine the coefficient of variance (COV) of the board surface temperature during heating in order to determine the point at which bubble birth began. A FLIR A20 camera (Thermovision A20 infrared camera operators manual, FLIR systems, Sweden, 2003.) with an uncooled microbolometer FPA detector was coupled to a lens with a $25^\circ \times 19^\circ$ field of view and a minimum focal distance of 0.3 m. This arrangement provides a thermal sensitivity of 0.12°C at 30°C. The system can analyze images at single pixel resolution and compensates for errors because of reflected radiation. Thermograms were taken by placing the board inside the oven; the camera was located outside the oven at a distance of 0.3 m from the object. The average temperature and standard deviations were measured for the area of interest for 120 s from the time the board was placed in the oven. The COV is the standard deviation of all of the temperatures in the area of interest divided by the average temperature. The standard deviation of temperatures measured across a unit area at different times was less than 4% for all the cases studied. The emissivity of the polymeric material was determined to be 0.97 by measuring the temperature of a black electric tape of known emissivity (0.96). The emissivity assigned to the board surface was adjusted so that the temperature of the board surface corresponded to the tape temperature. The IR camera was also used to confirm that the temperature of the polymer exceeded its melting point during foaming.

Results and Discussion

Typical SEM images of the cross-section of the board taken during foaming are illustrated in Figure 3 for a machine-made sheet; similar results were obtained for handsheets. Bubbles begin to grow at the paper/polymer interface (Figure 3a) and then expand into the polymer layer (Figure 3b). It is clear that a bubble originates at a pore, which implies that water vapor travels through the sheet structure, emerges at a pore opening and then foams the polymer. It follows, therefore, that the surface properties of the sheet, especially the pore distribution, will control the bubble profile of the finished product. Figures 3c and d illustrate a uniformly foamed board and a poorly foamed board, respectively. The water in the fiber is present at 6% by weight, which means that it covers the fiber surface as a monolayer.[9,10] At these low concentrations, nucleation of water vapor to form a vapor bubble is improbable. Transport of water into the polymer layer through simple flow of vapor through the pore is much more likely.

A representative example of a bubble growth profile is presented in Figure 4 and shows the time from which the first bubble appears in the video. On an average, the first bubble appeared at about 30 s from the time the sample was placed inside the oven. The bubble growth rate and the maximum number of bubbles are higher for the machine-made paper as compared to the handsheets. The maximum number of bubbles should directly correspond to the number of active pore openings that lead to bubble formation. The growth rate is related to the resistance offered by the porous sheet. The growth in bubble size and decay of the number of bubbles in the machine-made paper is due to bubble coalescence or bubble collapse. Figure 5 summarizes the maximum number of bubbles formed, the final bubble count at 90 s, and the degree of coalescence for several handsheets and a machine-made paper. The degree of coalescence was calculated from the maximum and final bubble count. There is a clear difference in the maximum number of bubbles and the degree

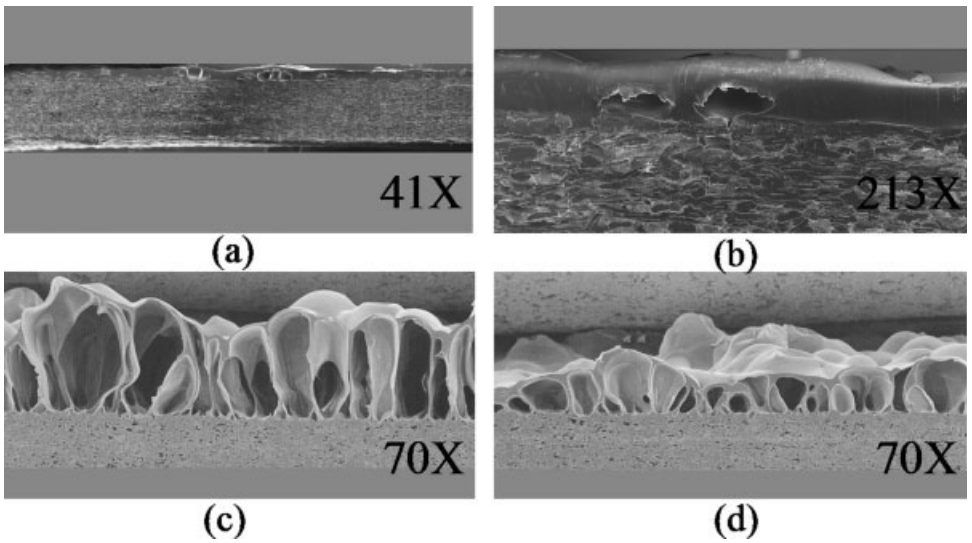

Figure 3. Bubble growth profiles and SEM analysis of cross sections; (a), (b) -after 10 s; (c), (d) -after 120 s.

of coalescence between the machine-made sheets and any of the handsheets. The higher degree of coalescence for the machine-made sheet is consistent with the larger number of bubbles initially formed. The higher bubble density would reduce the distance between bubbles and promote coalescence.

The behavior of the various handsheets was remarkably similar, despite the differences in fiber composition, the presence of additives, and the manner in which the sheets were prepared. A variation in these properties would be expected to change the number and size of pores present on the paper surface and also the internal structure of the porous web. These properties would also have varied any potential nucleation sites such as fiber surface defects, fiber–fiber crossings and the volume of air present (air bubbles). External nucleation agents are also frequently used in traditional polymer foaming.[11,12] Figure 6 compares bubble profiles of handsheets (H10 and H11) containing 5% clay with their clay-free counterparts. The clay had no effect on bubble distribution, confirming that nucleation is unimportant. Sheets H6 and H7 in Figure 5 were prepared in a Formette Dynamique where a multi-ply sheet is built up layer by layer and is, therefore, more stratified than the other laboratory-made sheets. Again, no differences in bubble profile were observed. The foaming behavior of sheets extruded on the felt (top) side and wire (bottom) side were also very similar. Clearly, bubble formation is relatively insensitive to the composition of the sheet and to at least some of the operational variables used to make it.

As the sheet warms up the moisture in the board evaporates and the water vapor enters the void space. As long as the volume density of the sheet remains constant the pressure developed within the sheet should be independent of the composition of the sheet. Foaming begins when the pressure builds up to the point where it overcomes the resistance of the molten polymer. The number of bubbles formed should

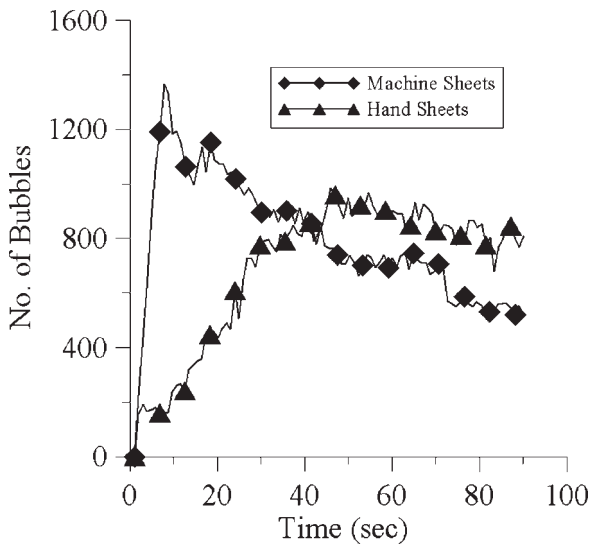

Figure 4. Growth profiles for laboratory handsheets and machine-made paper.

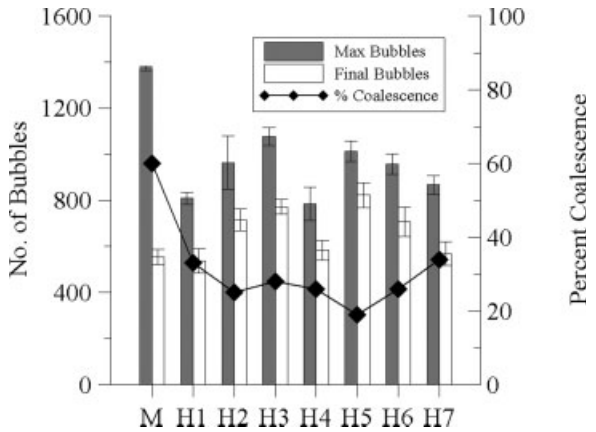

Figure 5. Variation of paper board properties in foaming.

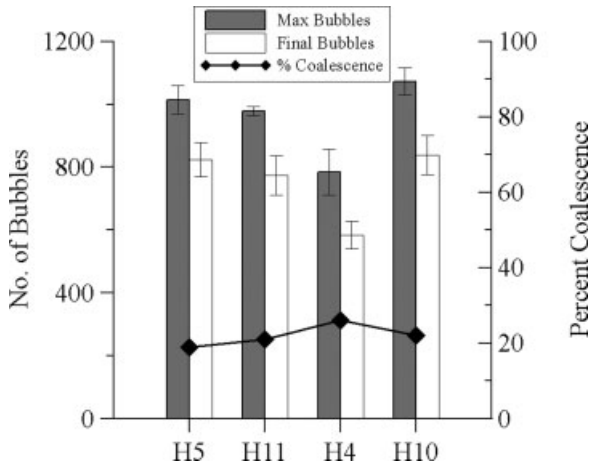

Figure 6. Effect of filler on foaming.

depend on the geometry of the surface of the sheet; well-distributed pores should lead to uniform bubbles. Thus, sheet uniformity should be the critical parameter governing bubble quality. The rate at which the vapor travels through the porous web should control the pressure build up, which governs the growth rate of the bubbles. This would depend on the resistance offered by the sheet to vapor transport.

To understand the differences in the surface profiles between the machine-made paper and the various handsheets, a new technique for studying the x–y surface uniformity of paperboard was used. An SEM image of the surface of the paperboard was taken before extrusion of the polymer. The image was converted to a 0–255 grayscale, ranging from the darkest to the brightest pixel, as illustrated in Figure 7. The dark regions represent the pores, while the gray regions represent the fiber surfaces. A surface uniformity index (SUI) was defined (Eq. 1) as the absolute difference between a given pixel and the mean pixel value of an image.

$$\text{Surface uniformity index (SUI)} = |(P - P*)| \qquad (1)$$

Here, P is the number of pixels times a given pixel value and P^* is the weighted mean, i.e., ΣP/(total number of pixels in the image). A higher SUI value indicates a greater deviation from the mean pixel value and represents a less uniform surface. Figure 8 shows the SUI plotted with respect to the different pixel values for both laboratory and machine-made samples. The machine-made sheets (M) show a lower SUI than any of the handsheets (H). This indicates that the machine-made sheets have better surface uniformity, i.e., a more uniform layout of the fibers and a more even pore distribution as compared to the handsheets.

If the board density remains constant, a more permeable sheet would lead to faster foaming. Results from air permeability measurements made with the Gurley Test[13] are shown in Figure 9. Samples M and H5 were prepared from the same furnish and had the same freeness values; as such they can be directly compared. The other handsheet samples are either of lower freeness or contain filler. The laboratory handsheets have a lower permeability compared to machine made sheets. The handsheets were prepared in the Formette unit where the sheet is constructed layer-by-layer. In contrast, in machine made paper a continuous jet of fiber and water is sprayed on the forming wire laying all of the fiber on the forming wire as a single layer. Although turbulence and drainage forces lead to some preferential positioning of filler and small fiber particles, the fiber arrangement is not significantly altered after deposition on the wire. Hence, the Formette handsheets should be more resistant towards vapor flow on account of its lower permeability. This results in slower foaming in the handsheets.

For foaming to begin pressure needs to build up inside the sheets. The time required for pressure build up is thus important in controlling the rate of foaming. The imaging experiments do not capture the start of foaming until the first bubble is developed to the point where it can be recognized as such by the camera. The build-up of vapor pressure depends both on the sheet permeability and on the rate at which the heat is transferred to the sheet. The point at which moisture exits the board to foam the polymeric layer should change the thermal conductivity of the polymer at the bubble surface and affect its temperature to a small degree. Representative thermograms taken of the board surface from laboratory and machine-made sheets led to the temperature profiles shown in Figure 10, which are very similar for the two

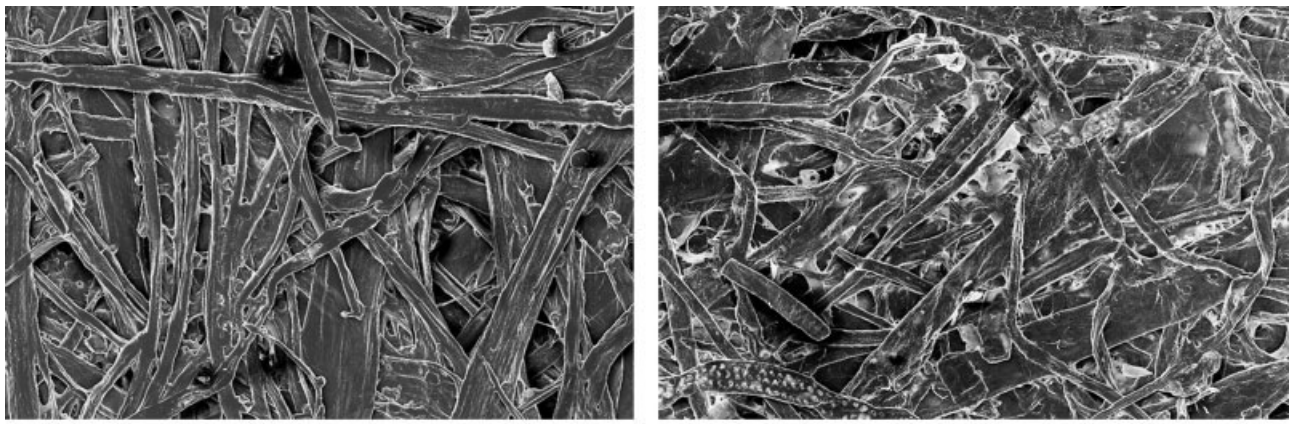

Figure 7. SEM images of samples M and H2.

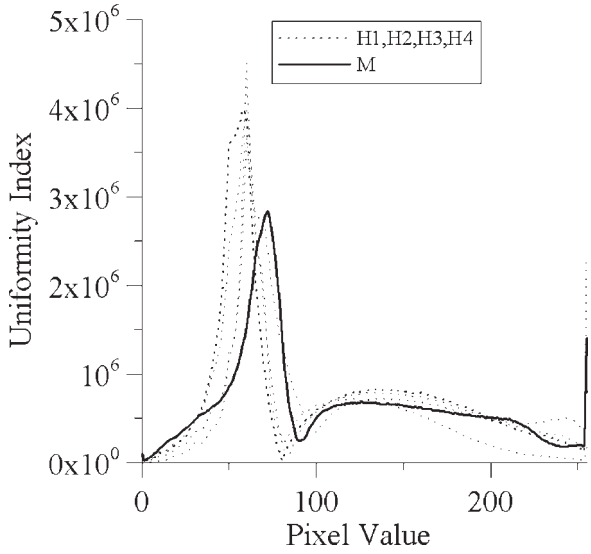

Figure 8. Variation in the uniformity index.

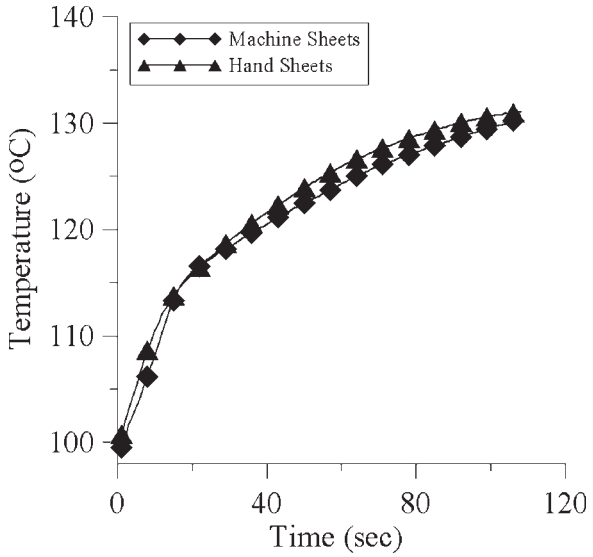

Figure 10. Temperature profiles of laboratory and machine-made sheets.

materials. Certainly, the difference in bubble formation seen in Figure 4 is not evident here.

A much larger difference is seen if the coefficient of variation (COV) of the temperature is considered instead of the temperature itself. We have shown earlier that the COV is a much more sensitive parameter than temperature for identifying subtle thermal effects, such as the point at which a surface just begins to dry.[14] In this example, "dry spots" begin to form on the surface and the variability in the surface temperature rises more sharply than the temperature itself. Figure 11 compares the representative COV profile for the machine-made sheets and the handsheets during the foaming process. In contrast to Figure 4, the time axis in Figures 10 and 11 starts from the point at which the sample was placed inside the oven. For the machine-made sheets, the COV decreases initially because of the increase in temperature uniformity across the surface. The onset of foaming causes nonuniformities in temperature and thus increases the COV. Thus, the lowest value of COV (at 24 s) is believed to signal the start of the foaming process. The handsheets show an initial increase in COV in the first few seconds. The less uniform surface of a handsheet causes nonuniform heating leading to the initial increase. Upon further heating, the temperature uniformity increases and reduces the COV. However, this decrease is more gradual than that for the machine-made sheets. This implies a slower build up of pressure leading to a slower foaming process as observed in the imaging experiments. Since the heating rates for the two sheets were similar, the lower permeability of the hand sheets is the reason for the slower growth rate observed.

Traditional foaming, a process well studied in literature[1–3,15–18] involves saturating the polymer with a blowing agent under high pressure. A further reduction in pressure

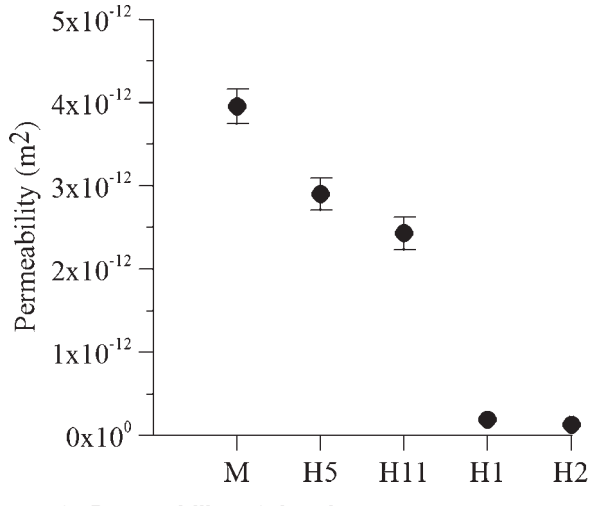

Figure 9. Permeability of the sheets.

Error bars are only provided for situations where the standard deviation exceeds 1%.

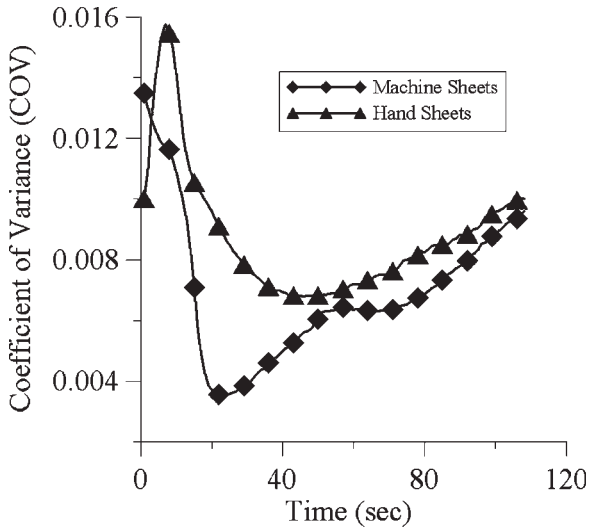

Figure 11. Coefficient of variance of temperature profiles.

leads to nucleation of dense gas bubbles (blowing agent) in the polymeric melt solution. These bubbles, in turn, grow to form the foam structure. The foam quality is in effect dictated by the nucleation kinetics and the bubble growth dynamics. Several factors could affect such a process including temperature, pressure, nucleating agents, melt rheology, and solubility of the blowing agent. In contrast, foaming of polymer-laminated paperboard is dictated by the ability of the moisture to travel to and escape from the pores on the surface of the sheet into the molten polymeric layer. The Uniformity Index and the COV results both implicate surface uniformity as the parameter responsible for the difference in behavior between the machine-made and the handsheets. The uniformity of the distribution of pores appears to be critical. Evenly sized and spaced pores will give rise to well-distributed bubbles in the foamed product. Thus, the sheet structure is critical to product uniformity.

In conclusion, we have demonstrated that the foam quality of polymer/paperboard composites depends (in part) on the pore distribution of the paperboard surface. Water vapor from the board escape through these pores and foam the polymer face, so that the final foamed structure depends on the pore distribution on the surface of the underlying paperboard. This technique is currently being expanded to foam biodegradable polymers on paper to serve as an environmental friendly solution. Although the present work uses paperboard as the base substrate for foaming, the technique could also be applied to any porous substrate.

Acknowledgment

Kiran Annapragada was supported by a fellowship from Institute of Paper Science and Technology.

Literature Cited

1. Lee ST, Ramesh NS. *Polymeric foams: mechanisms and materials*. Boca Raton: CRC press, 2004.
2. Feng JJ, Bertelo CA. Prediction of bubble growth and size distribution in polymer foaming based on a new heterogeneous nucleation model. *J Rheol*. 2004;48:439–462.
3. Colton JS, Suh NP. The nucleation of microcellular thermoplastic foam with additives. I. Theoretical consideration. *Polym Eng Sci*. 1987;27:485–492.
4. Iioka A. Method for producing a heat-insulating paper container from a paper coated or laminated with a thermoplastic synthetic resin film. US Pat. 4435344, 1984.
5. Waterhouse JF. Effect of some papermaking variables on formation. IPST technical paper series Number 438, 1992.
6. Fleischman EH Jr. An investigation of the elastic and dielectric anisotropy of paper. PhD Thesis. Institute of Paper Science and Technology, Atlanta, GA, 1981.
7. TAPPI T402 sp-03. Standard conditioning and testing atmospheres for paper, board, pulp handsheets, and related products, 2007.
8. Rasband WS. Image J. National Institutes of Health. Bethesda, Maryland, USA. (Available at: http://rsb.info.nih.gov/ij/.1997–2004).
9. Walsh FL, Banerjee S. Characterization of thin water layers in pulp by tritium exchange. I. Methods development. *Holzforschung*. 2007;61:115–119.
10. Hernadi A. Accessibility and specific surface of cellulose measured by water vapor sorption. *Cellulose Chem Technol*. 1984;18:115–124.
11. Park CB, Cheung KL, Song SW. The effect of talc on cell nucleation in extrusion foam processing of polypropylene with CO2 and isopentane. *Cell Polym*. 1998;17:221–251.
12. Rodrigue D, Gosselin R. *The effect of calcium carbonate particle size on LDPE foam morphology*. In: Blowing Agents and Foaming Processes Conference, Heidelberg, 2002:157–166.
13. Knauf GH, Doshi MR. Calculations of aerodynamic porosity, specific surface area and surface volume from Gurley seconds measurements. Institute of Paper Chemistry Technical Paper Series No. 183, 1986.
14. Fike GM, Abedi J, Banerjee S. Imaging the drying of surfaces by infrared thermography. *Ind Eng Chem Res*. 2004;43:4178–4181.
15. Lee ST, Park CB, Ramesh NS. *Polymeric foams: science and technology*. Boca Raton: CRC press, 2007.
16. Ramesh NS, Rasmussen DH, Campbell GA. The heterogeneous nucleation of microcellular foams assisted by the survival of micro voids in polymers containing low glass transition particles. I. Mathematical modeling and numerical simulation. *Polym Eng Sci*. 1994;34:1685–1697.
17. Amon M, Denson CD. A study of the dynamics of foam growth: analysis of the growth of closely spaced spherical bubbles. *Polym Eng Sci*. 1984;24:1026–1034.
18. Joshi K, Lee GL, Shafi MA, Flummerfelt RW. Prediction of cellular structure in free expansion of viscoelastic media. *J Appl Polym Sci*. 1998;67:1353–1368.

Manuscript received July 21, 2007, and revision received Oct. 28, 2007.